Spectral and temporal holograms with nonlinear optics

Roy Shiloh* and Ady Arie

Department of Physical Electronics, Fleischman Faculty of Engineering, Tel Aviv University, Tel Aviv 69978, Israel
**Corresponding author: royshilo@post.tau.ac.il*

Received June 6, 2012; accepted July 13, 2012;
posted July 16, 2012 (Doc. ID 170019); published August 24, 2012

In this Letter we show how encoding techniques for computer-generated holograms may be used to arbitrarily shape a nonlinearly generated spectrum and consequently the temporal shape by modulating the quadratic nonlinear coefficient. We give examples of a modulation pattern and a simple setup that can generate high-order Hermite–Gauss and Airy functions through difference-frequency generation from a transform-limited Gaussian pulse, under practical fabrication considerations. © 2012 Optical Society of America

OCIS codes: 190.0190, 190.4410, 090.0090, 090.6186.

The concept of computer-generated holograms (CGHs) conventionally allows designing a slide that stores the amplitude and phase of a wavefront, which may later be reconstructed by illuminating the hologram with a reference beam. When interest in holographic techniques grew in the 1960s, different authors proposed different coding techniques [1–3]. In an article by Lee [4], a general and accurate method for the design of a binary CGH was developed. In essence, given the complex representation of the Fourier transform of the object wave to be recorded, $u(x,y) = A(x,y)\exp[i\varphi(x,y)]$, the binary CGH transmission is prescribed by

$$t(x,y) = \text{sign}\{\cos[2\pi f_c x + \varphi(x,y)] - \cos[\pi q(x,y)]\}, \quad (1)$$

where f_c, the carrier frequency, is the periodic grating frequency upon which the information is modulated using the object wave's phase $\varphi(x,y)$ and amplitude $A(x,y)$, where by setting $\sin \pi q(x,y) = A(x,y)$ the object wave is obtained in the first diffraction order.

Recent advances in CGH research incorporated nonlinear optics; in this so-called "nonlinear CGH," the quadratic nonlinear coefficient is modulated, thereby allowing us to convert a fundamental Gaussian beam into a second-harmonic beam with a desired wavefront [5,6]. In this Letter we further extend nonlinear CGHs from the spatial domain to the spectral domain, arbitrarily shaping the spectrum of the generated pulse, and, owing to the Fourier transform relation between the spectrum of a pulse and its temporal shape, this also enables one to shape the nonlinearly generated pulse in time.

In nonlinear quadratic optics, we assume a process of difference-frequency generation (DFG) involving the complex amplitudes of a narrow pump [quasi-continuous wave (quasi-CW)] A_1, a spectrally broad input pulse A_2, and a generated wave A_3. Approximating the pump and input pulse as undepleted, the generated wave is the Fourier transform of $d(z)$ [7]:

$$A_3 = \kappa \int_{-\infty}^{\infty} d(z) e^{i\Delta k z} \mathrm{d}z, \quad (2)$$

where the phase mismatch is $\Delta k = k_1 - k_2 - k_3$ and κ includes A_1 and A_2—a linear relation between the pump and input waves to the difference-frequency wave (a comprehensive discussion is available in [8]). Equation (1) is interpreted so as to describe the generated spectrum after propagation in a nonlinear medium with a given phase mismatch Δk:

$$A_3(\Delta k) = \kappa \int_{-\infty}^{\infty} \text{IFT}\{D(\Delta k)\} e^{i\Delta k z} \mathrm{d}z, \quad (3)$$

where $d(z) = \text{IFT}\{D(\Delta k)\}$ clearly states the inverse Fourier transform relationship between the spatial nonlinear modulation $d(z)$ and its spectral shape, $D(\Delta k)$. A similar result may be derived for sum-frequency generation; conversely, in a second-harmonic process, κ would include the square of the fundamental complex amplitude, A_1^2, or more accurately its self-convolution [9], which complicates the treatment and design of the nonlinear CGH. Hence, we will only consider here as an example the process of DFG.

We may now incorporate the nonlinear CGH into the nonlinear scheme. The carrier frequency is chosen to efficiently phase match the nonlinear process, so $f_c = \Delta k_0/2\pi$, and Δk_0 is the phase mismatch of the central frequency. This choice of f_c imposes a limit on the bandwidth B of the encoded signal; if, in the first diffraction order, the signal spans $\Delta k_0 \pm 0.5B$, then to avoid overlap with the second diffraction order we require that [1]

$$B < \frac{2\Delta k_0}{3}. \quad (4)$$

The object wavefront $u(x,y)$, a transverse function, is replaced by the inverse Fourier transform of the spectral modulation function $U(\Delta k)$, along the propagation axis, so $u(z) = A(z)\exp[i\varphi(z)] = \text{IFT}\{U(\Delta k)\}$. Now the nonlinear modulation along the propagation axis is

$$d(z) = d_{ij}\text{sign}\{\cos[\Delta k_0 z + \varphi(z)] - \cos[\pi q(z)]\}, \quad (5)$$

where again $\sin \pi q(z) = A(z)$ and d_{ij} is an element of the quadratic susceptibility tensor. The analogy is therefore simple and apparent: the nonlinear process is effectively a Fourier transform between the spatial domain and the spectral domain, and the nonlinear CGH is coded in such a way as to reconstruct the desired, arbitrary shape, in the nonlinearly generated spectrum.

As an interesting example, we demonstrate amplitude modulation by encoding the ninth-order Hermite–Gauss function (HG09), given by [10]

0146-9592/12/173591-03$15.00/0

$$G(\zeta) = H_9(\zeta)e^{-\zeta^2/2}, \quad (6)$$

where $H_9(\zeta)$ is the ninth-order Hermite polynomial, $\zeta(z) = \sqrt{2}z/\omega(z)$ is a scaled propagation parameter, and $\omega(z) \approx \omega_0$ is the conventionally defined e^{-1} Gaussian radius, which is approximately constant in z for our purposes. Since HG functions are shape invariant under the Fourier transform, $U(\Delta k)$ would also be HG09. Spatially, we set $\omega_0 = L/10$, where L is the nonlinear interaction length, so the modulation extends throughout it, and the amplitude's FWHM $[|G(\zeta)| = 0.5]$ is estimated by $b = \omega_0 \times 3.837 \times 2\sqrt{\ln 2}$, where 3.837 is a numerically found width correction factor for a ninth-order HG mode. For the definition in Eq. (6), the spectral B is related to the spatial b according to $B = b/(\omega_0^2/2)$, so the spectral overlap condition in Eq. (4) becomes $\omega_0 \gg 6.389/\Delta k_0$, where a stricter condition is applied since b is defined as FWHM while B is a rigid window. This condition is satisfied for all practical selections of ω_0 (in terms of manufacturing capabilities), since in nonlinear (DFG) interactions in the near IR Δk_0 is usually of the order of 10^5–10^7 m^{-1}.

We simulate a pump laser at 532 nm, a transform-limited Gaussian input pulse of 77 fs FWHM centered around 810 nm to produce a spectral FHWM of 25 nm, and a nonlinear crystal, which manifests a DFG process. To enhance the nonlinear process and minimize the effects of group velocity mismatch (GVM), we first stretch the input pulse to 0.5 ns using, for example, a dispersive medium such as a fused silica fiber [11] of length $L_s \approx$ 196.5 m (here we only included terms up to the second-order derivative of the refractive index, so the input pulse group velocity dispersion is 35 fs^2/mm). Both pump and chirped input pulses are then fed into a nonlinear crystal with modulated nonlinearity, which may be realized, for example, by electric-field poling of ferroelectric crystals, e.g., potassium titanium oxide phosphate [12]. These parameters yield $\Delta k_0 = 6.57 \times 10^5$ m^{-1} at 100 °C crystal temperature (setup depicted in Fig. 1). To produce a sharper spectral acceptance, the crystal length is $L =$ 40 mm, and we assume a minimum domain size of $\Delta z =$ 345 nm, in agreement with recent experimental results [13]. Finally, to further bolster our argument of neglecting GVM-related effects, we calculate the input-to-output GVM, 7.7 ps/40 mm, and alternatively show that the dispersion length is adequately long, $L_D = \Delta\tau/\mathrm{GVM} =$ 2.6 m $\gg L$.

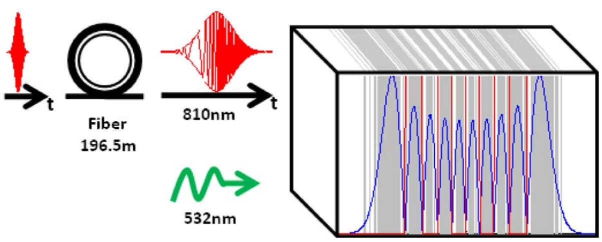

Fig. 1. (Color online) Generating HG09 spectrum: an input transform-limited 77 fs Gaussian pulse around 810 nm is stretched to 0.5 ns and fed together with a quasi-CW 532 nm pump into an HG09-encoded nonlinear CGH. In-crystal curves: modulated domains (gray), amplitude (blue), and phase (red) of the encoded CGH.

We use the split-step Fourier beam propagation method along the z axis to simulate the nonlinear process, which produces an output, the DFG pulse, set around 1550 nm. The amplitude modulation we performed is unaffected by the pulse chirp, and the HG09 function is readily evident at the crystal output facet, measuring 115.6 ps and 21.2 nm FWHM. Both spectral and temporal representations of the DFG pulse are depicted in Fig. 2, qualitatively showing an excellent reproduction of the encoded pattern. We note that, consequently to the HG09 shape invariance, even if the DFG pulse is compressed or further stretched, the temporal shape remains HG09 (though its width will change).

Next, we will employ the finite Airy function [14], which was previously manifested optically through use of a cubically modulated grating both linearly [15] and nonlinearly [16], to generate a pulse whose spectrum is in the form of the Airy function. We employ the same setup, replacing the HG09 CGH with an encoded cubic phase multiplied by a Gaussian envelope (see Fig. 3):

$$u_2(\zeta(z)) = e^{i\pi p \times \zeta^3 (z/2\sqrt{2\ln 2})} e^{-\zeta^2(z)/2}, \quad (7)$$

where $\zeta(z)$ is defined as before and $p = 10$ relates the phase accumulation in multiples of 2π to $b = \omega_0 \times 2\sqrt{\ln 2}$, the Gaussian envelope's FWHM. We choose $\omega_0 = L/5$ so the Gaussian amplitude adequately fills the available interaction length. In terms of spectral overlap, a stricter condition than Eq. (4) may be derived [1] since the resultant spectral Airy is not symmetric around Δk_0. However, in our case and in practice, we relax this condition since it is satisfied for most practical selections of b and p. To this end, we approximate the Airy spectral width with a Gaussian function [dashed blue curve in Fig. 4(a)]:

$$G(\Delta k) = e^{-\left(\frac{\Delta k - \Delta k_0}{2(1+2p)/\omega_0}\right)^2}, \quad (8)$$

$$B = 8(1 + 2p) \times \ln 2/b, \quad (9)$$

where B is its spectral FWHM; this form converges with the case of an amplitude-only Gaussian modulation, $p = 0$, and intersects the Airy tail's declining trend at roughly 1% of its height, a limit controlled by the coefficient of p (in this case, 2). The condition in Eq. (4) may now be approximated as $\omega_0 \gg 5(1 + 2p)/\Delta k_0$, which is satisfied here, since $\omega_0 = 8$ mm $\gg 0.77$ mm.

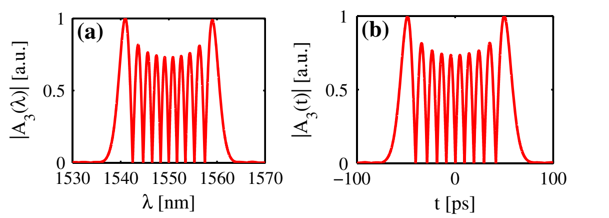

Fig. 2. (Color online) DFG wave at crystal output shows the reconstructed (a) spectral HG09 measuring 21.2 nm FHWM and (b) its representation in time, measuring 115.6 ps.

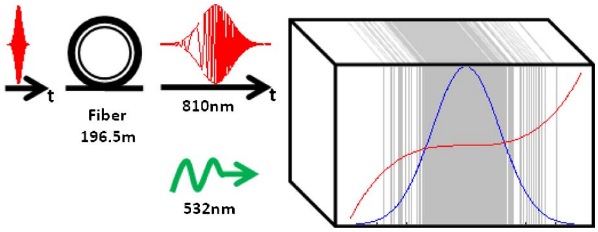

Fig. 3. (Color online) Generating Airy spectrum: a pump and stretched input pulse are fed into a nonlinear crystal, where the encoded nonlinear CGH is a cubically phased Gaussian amplitude (the Fourier transform of is, of course, the finite Airy function). In-crystal curves: modulated domains (gray), amplitude (blue), phase (red) of the encoded CGH.

In Fig. 4 we observe the DFG pulse at the crystal end facet. As soon as it exits the crystal, the nonlinear interaction ceases, and a spectral Airy is fixed [see Fig. 4(a)], the phase of which comprises mainly delay and chirp introduced by the stretching of the input pulse. This large accumulated quadratic phase creates a mathematical frequency-to-time mapping through the Fourier transform relationship [17] as evident in Fig. 4(b). We emphasize that, while the pulse resembles the Airy in shape, it is not a shape-invariant pulse since its spectral phase does not have a pure cubic dependence. Hence, its width and direction depends mainly on the stretching fiber's length (or amount of accumulated quadratic phase).

With the apparent ease in which the spectrum can be shaped, one may propose shaping light in both spectral and spatial domains, creating "light bullets" [18] with a compact setup. Such light bullets, spatiotemporal optical wave packets, would remain unaffected by dispersion and diffraction. The methods discussed in this Letter combined with the design from [16] could generate a nonlinear Airy (in space)–Airy (in time) light bullet.

In conclusion, we have shown that the method of encoding a CGH, which has previously been used for spatial shaping, can analogously be exploited for spectral shaping in nonlinear optics. We gave two examples describing the encoding and generation of an HG09 and of a cubic phase to generate an Airy in the spectrum. While implementation may not yet be straightforward, the proposed nonlinear spectral holograms satisfy the current fabrication limitations of electric-field poling in ferroelectrics. The application of well-based methods for creating a

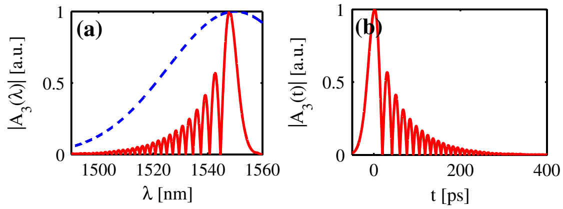

Fig. 4. (Color online) DFG pulse at the crystal output. (a) Spectral representation showing an Airy function (red) and the Gaussian approximation of its width [Eq. (8), dashed blue curve]; (b) temporal representation, exhibiting a frequency-to-time mapping.

CGH is a valuable asset that may open new opportunities for spectral and temporal shaping and manipulation.

This work was supported by the Israel Science Foundation.

References

1. E. Wolf, in Vol. XVI of *Progress in Optics* (North-Holland, 1978), Chap. 3.
2. B. R. Brown and A. W. Lohmann, Appl. Opt. **5**, 967 (1966).
3. J. J. Burch, Proc. IEEE **55**, 599 (1967).
4. W. Lee, Appl. Opt. **18**, 3661 (1979).
5. A. Shapira, I. Juwiler, and A. Arie, Opt. Lett. **36**, 3015 (2011).
6. A. Shapira, R. Shiloh, I. Juwiler, and A. Arie, Opt. Lett. **37**, 2136 (2012).
7. R. W. Boyd, *Nonlinear Optics*, 3rd ed. (Academic, 2008).
8. G. Imeshev, M. M. Fejer, A. Galvanauskas, and D. Harter, J. Opt. Soc. Am. B **18**, 534 (2001).
9. G. Imeshev, M. A. Arbore, M. M. Fejer, A. Galvanauskas, M. Fermann, and D. Harter, J. Opt. Soc. Am. B **17**, 304 (2000).
10. B. E. A. Saleh and M. C. Teich, in *Fundamentals of Photonics* (Wiley, 1991), Chap. 3.
11. I. H. Malitson, J. Opt. Soc. Am. **55**, 1205 (1965).
12. K. Fradkin, A. Arie, A. Skliar, and G. Rosenman, Appl. Phys. Lett. **74**, 914 (1999).
13. A. Zukauskas, G. Strömqvist, V. Pasiskevicius, F. Laurell, M. Fokine, and C. Canalias, Opt. Mater. Express **1**, 1319 (2011).
14. G. A. Siviloglou and D. N. Christodoulides, Opt. Lett. **32**, 979 (2007).
15. G. A. Siviloglou, J. Broky, A. Dogariu, and D. N. Christodoulides, Phys. Rev. Lett. **99**, 213901 (2007).
16. T. Ellenbogen, N. Voloch-Bloch, A. Ganany-Padowicz, and A. Arie, Nat. Photonics **3**, 395 (2009).
17. A. Papoulis, in *Signal Analysis* (McGraw-Hill, 1977), Chap. 8.
18. A. Chong, W. H. Renninger, D. N. Christodoulides, and F. W. Wise, Nat. Photonics **4**, 103 (2010).